PHYSICAL REVIEW A **92**, 061603(R) (2015)

Crystallization of a dilute atomic dipolar condensate

R. N. Bisset and P. B. Blakie
Dodd-Walls Centre for Photonic and Quantum Technologies, Department of Physics, University of Otago, Dunedin, New Zealand
(Received 30 October 2015; published 29 December 2015)

We present a theory that explains the experimentally observed crystallization of a dilute dysprosium condensate into a lattice of droplets. The key ingredient of our theory is a conservative three-body interaction which stabilizes the droplets against collapse to high-density spikes. Our theory reproduces the experimental observations, and provides insight into the many-body properties of the droplet phase. Notably, we show that it is unlikely that a supersolid was obtained in experiments, however, our results suggest a strategy to realize this phase.

DOI: 10.1103/PhysRevA.92.061603 PACS number(s): 67.85.Hj, 67.80.K−

Recent experiments with ultracold dysprosium [1] have observed the crystallization of a superfluid into a regular array of droplets. This result is surprising because it realizes a droplet crystal, which has been the subject of considerable theoretical work, yet avoids much of the complex interaction engineering in existing proposals, e.g., using ensembles of cold Rydberg atoms [2,3] or polar molecules [4]. However, the standard theoretical description of dysprosium condensates does not predict a stable droplet phase, suggesting the role of additional physics. In this Rapid Communication, we propose that this additional physics arises from a conservative three-body interaction (e.g., see Ref. [5]). Augmenting the standard theory with this term, we show that a stable droplet crystal forms (e.g., see Fig. 1) and we are able to explain the main observations made in the experiment [1]. We note that this type of interaction has been found to play a dominant role in recent experiments with ^{85}Rb [6].

Dysprosium has a large magnetic moment giving rise to a significant long-ranged dipole-dipole interaction (DDI) between the atoms. In the experiment [1] it is necessary to enhance (via Feshbach resonance) the short-range repulsive interaction to be comparable in strength to the DDI in order to produce the initial (unstructured) condensate. The crystallization is then initiated by suddenly reducing the value of the short-range interaction, allowing the condensate to evolve with a dominant DDI. Detailed observations of the crystallization dynamics are revealed by the use of high-resolution *in situ* imaging of the system. Key experimental observations include the following: (i) The droplets form into an approximately triangular lattice with lattice constants in the range 2–3 μm and that persist for long times ($\gg$100 ms, although with some droplet dynamics); (ii) the lattice formation time is $\sim$7 ms after the interaction quench; and (iii) the number of droplets formed is stochastic, but, on average (over the range studied), the average droplet number increases linearly with condensate number.

Because the system we consider is dilute, its dynamics should be well described by the mean-field Gross-Pitaevskii theory. This theory includes short-range (contact) and long-range (dipole-dipole) two-body interactions [7], and has been successful at describing a range of equilibrium and dynamic phenomena, such as the parameter regions where the condensate is mechanically stable [8,9] and collapse dynamics [7,10]. However, this theory applied to the experimental scenario outlined above fails to describe the observed dynamics: Mean-field theory predicts that the system is unstable to forming sharp infinite-density spikes [11], in which regime the mean-field description is invalid. Indeed, such mechanical collapse scenarios are usually accompanied by explosive dynamics, rapid atom loss, and heating (e.g., see Refs. [7,12,13]). Hence, the observation of regular, stable, and long-lived droplets in the dilute regime indicates the presence of additional physics not included in the standard theory.

Three-body recombination is an important loss mechanism in experiments which occurs when three ultracold atoms collide to form a diatomic molecule and an atom that are both lost from the atom trap. The measurement of the three-body recombination rate has been used to reveal quantum statistical and many-body effects (e.g., see Refs. [14,15]), and to locate Feshbach resonances (e.g., see Ref. [16]). There is also a conservative three-body interaction between the particles, which does not lead to loss [5], and is expected to be large if there is an Efimov state near the collision threshold [17,18]. While we are not aware of any quantitative predictions for three-body interactions in ^{164}Dy, this atom is known to have complex collisional properties, including a large number of Feshbach resonances [16]. Since ultracold atomic systems are so dilute, the role of such three-body interactions is typically much smaller than the two-body interactions. However, in scenarios where the system becomes mechanically unstable, due to attractive two-body interactions, the density can increase significantly and three-body terms can be important [18]. Indeed, a recent experiment with ^{85}Rb [6] has measured a conservative three-body interaction that is two to three orders of magnitude larger than the three-body recombination rate. Here, we show that by including a three-body interaction of comparable size we are able to quantitatively describe the crystallization observed in the dysprosium experiments.

To perform simulations we take the system evolution to be described by the Gross-Pitaevskii equation (GPE)

$$i\hbar\frac{\partial\psi}{\partial t} = \left[H_{\rm sp} + \int d\mathbf{r}'\, U(\mathbf{r}-\mathbf{r}',t)|\psi(\mathbf{r}',t)|^2 + \frac{\kappa_3}{2}|\psi|^4\right]\psi, \tag{1}$$

where $H_{\rm sp} = -\hbar^2\nabla^2/2m + V_{\rm trap}$, and

$$U(\mathbf{r},t) = \frac{4\pi\hbar^2 a(t)}{m}\delta(\mathbf{r}) + \frac{\mu_0\mu^2}{4\pi}\frac{1-3\cos^2\theta}{r^3} \tag{2}$$

describes the two-body contact and dipolar interactions for dipoles polarized along z, with θ being the angle between $\mathbf{r}$ and the z axis. Here, m is the atomic mass and $\mu = 9.93\mu_{\rm B}$

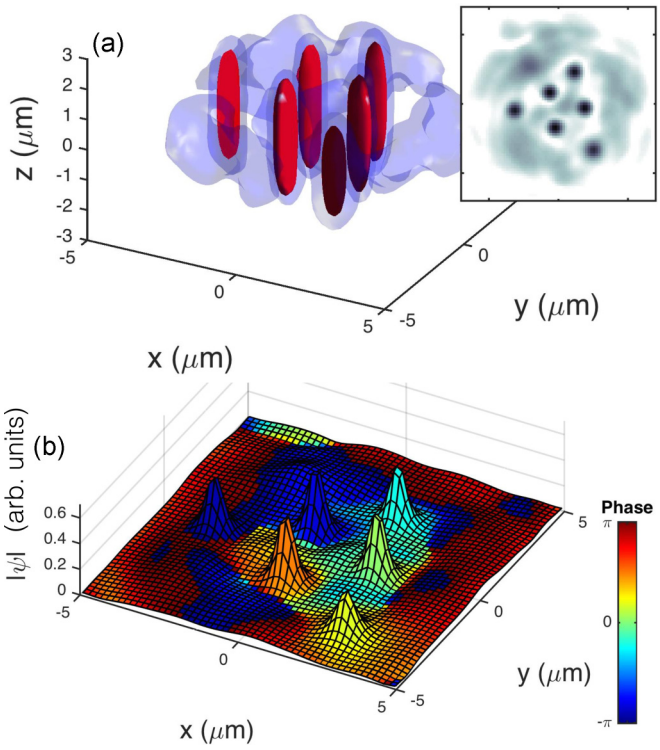

FIG. 1. (Color online) (a) Droplet crystal obtained in our simulations at $t = 15$ ms after the quench is started. The red surface indicates a high-density isosurface at $n = 2 \times 10^{20}$ m^{-3} and the blue low-density isosurface is $n = 0.2 \times 10^{20}$ m^{-3}. The inset is a column density made by integrating the density along the z axis. (b) Condensate phase in the $z = 0$ plane. Simulation for $N_{\rm cond} = 15 \times 10^3$, $T = 20$ nK, and $(\kappa_r,\kappa_i) = (5.87 \times 10^{-39}, 7.8 \times 10^{-42})\hbar$ m^6/s, with other parameters as discussed in the text.

is the magnetic moment of a Dy atom, with $\mu_{\rm B}$ the Bohr magneton. The two-body contact interaction, parametrized by the s-wave scattering length $a(t)$, is time dependent as it is changed using a magnetic Feshbach resonance. The last term in (1) describes short-ranged three-body interactions. The coefficient is complex, $\kappa_3 = \kappa_r - i\kappa_i$, with κ_r characterizing the strength of the conservative component and κ_i quantifying the three-body recombination loss rate.

We perform simulations in the regime reported in Ref. [1] and consider condensates up to $N_{\rm cond} = 20 \times 10^3$ atoms prepared in a harmonic trap ($V_{\rm trap}$) with frequencies $(\nu_x,\nu_y,\nu_z) = (45,45,133)$ Hz and with the dipoles polarized along the z axis. The condensate is initially prepared with a scattering length of $a_i = 130a_0$, where a_0 is the Bohr radius. This value is obtained using a Feshbach resonance in the experiment, and ensures that a stable (unstructured) condensate is produced.

We take the initial condensate $\psi_0(\mathbf{r})$ to be the stationary solution of Eq. (1) normalized to $N_{\rm cond}$ with $\kappa_3 = 0$, which we solve for by using a Newton-Krylov scheme [19,20]. We note that the effect of the κ_r values we use for dynamics is negligible in the initial state (with peak density of $\sim 0.91 \times 10^{20}$ m^{-3} for $N_{\rm cond} = 15 \times 10^3$), making less than a 1% change in the ground-state energy. Thus, taking $\kappa_r = 0$ for the initial-state preparation is a good approximation. To the condensate we add initial-state fluctuations to account for quantum and thermal fluctuations in the system. Such fluctuations play an essential role in the droplet formation dynamics and are added as

$$\psi(\mathbf{r},0) = \psi_0(\mathbf{r}) + \sum_n{}' \alpha_n \phi_n(\mathbf{r}), \tag{3}$$

where $\epsilon_n\phi_n = H_{\rm sp}\phi_n$ are the single-particle eigenstates, α_n is a complex Gaussian random variable with $\langle|\alpha_n|^2\rangle = (e^{\epsilon_n/k_BT} - 1)^{-1} + \frac{1}{2}$, and the sum in (3) is restricted to modes with $\epsilon_n \leqslant 2k_BT$. This choice of fluctuations is made according to the truncated Wigner prescription (see Ref. [21]) for a system at temperature T. The main results we present are for $T = 20$ nK, adding approximately 400 atoms to the system, consistent with the experimental conditions of a "quasipure condensate" (cf. the ideal condensation temperature of $T_c = 72$ nK for $N = 15 \times 10^3$). For dynamics we evolve the system according to the GPE (1) discretized on a three-dimensional grid in a cubic box of dimension 23.4 μm, propagated in time using a fourth-order Runge-Kutta integration method. The number of grid points is varied to check the accuracy of results. The kinetic energy term is evaluated in Fourier space for spectral accuracy, and the DDI term is evaluated using fast Fourier transforms to perform the convolution, with a spherically cutoff dipole kernel used in k space to minimize the boundary effects [19]. The three-body interaction only plays an important role in the dynamics when the density gets high and we choose to use a constant value of κ_3 throughout each simulation.

The s-wave scattering length is linearly ramped from a_i to a_f over 0.5 ms, and then held constant for the remainder of the simulation. As in experiment, we consider a quench to a_f, close to the background value $a_{\rm bg}$, which initiates the crystallization. There remains appreciable uncertainty in the value of $a_{\rm bg}$ with the current experimental estimates being $92(8)a_0$ [16,22]. Having explored a range of simulation parameters, we find dynamics similar to experiment for $a_f \approx 82.6\,a_0$ [23]. At this value the condensate is susceptible to the growth of unstable modes [24–26]; these lead to the development of high-density regions near the trap center (i.e., local collapse [9,11]), and then across the condensate, driven by the attractive component of the DDI. On a time scale of 5–15 ms (depending on parameters), several high-density droplets form and the role of κ_3 becomes crucially important [e.g., see Fig. 2(c)].

We automate droplet detection in our simulations by identifying local column-density maxima (with densities exceeding $1.2\times$ the peak density of the initial condensate). We identify the region about this point where the density decays to define the droplet. We note (e.g., see Fig. 1) that once the droplets fully form, they deplete the atomic density at their boundaries and are thus unambiguously identified.

In Fig. 2(a) we show results for the number of droplets that are identified at 20 ms after the quench begins as a function of the atom number. Results are from five calculations at each atom number, and with an initial temperature of $T = 20$ nK, and we take $(\kappa_r,\kappa_i) = (5.87 \times 10^{-39}, 7.8 \times 10^{-42})\hbar$ m^6/s. The value of κ_i was chosen to ensure that the lifetime (decay of total number) in the droplet crystal was comparable to the value of 300 ms measured in experiments. The initial droplet formation and droplet properties are otherwise independent of κ_i. Because of the different initial noise, the number of droplets that form vary from run to run. Our results are similar to the

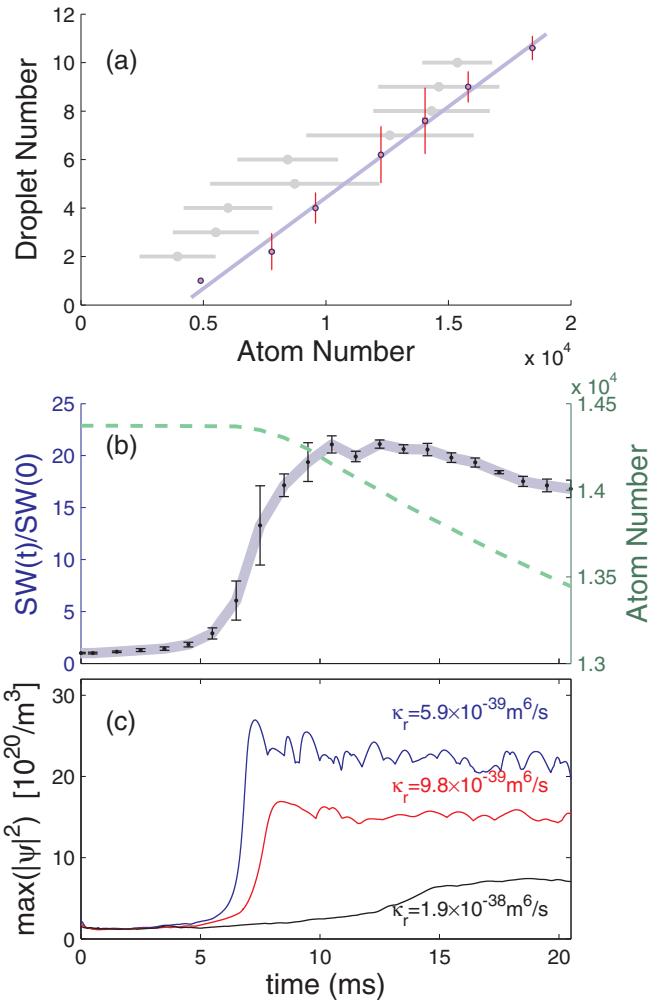

FIG. 2. (Color online) Droplet formation. (a) Number of droplets vs total atom number averaged over five simulations for each case. The line is best fit with slope 7.50×10^{-4}. The light gray circles with horizontal error bars are the experimental results from Ref. [1]. (b) Symbols with error bars indicate the relative spectral weight vs time and the dashed line shows the total atom number. (c) Peak density for simulations with different κ_r values. In all cases, $T = 20$ nK and $\kappa_i = 7.8 \times 10^{-42}\ \hbar\ \mathrm{m}^6/\mathrm{s}$. In (a) and (b), $\kappa_r = 5.87 \times 10^{-39}\ \hbar\ \mathrm{m}^6/\mathrm{s}$. In (b) and (c), $N_{\mathrm{cond}} = 14 \times 10^3$.

experimental measurements [1], except that the experimental measurements tend to find more droplets forming for 5×10^3 atoms, which may indicate that either a_f is lower than we use, or our criteria for identifying droplets are different.

Following the experiment, we evaluate a spectral weight to quantify the spatial structure in the *in situ* column density images on μm length scales postquench. This is done in terms of the function $\mathrm{SW}(t) = \sum_k' S_t(k)$, where $S_t(k)$ is the radially averaged Fourier transform of the column density (along z) at time t, with the sum taken over the range $k \in [1.5,5]\ \mu\mathrm{m}^{-1}$. The relative spectral weight, $\mathrm{SW}(t)/\mathrm{SW}(0)$, is a measure of the increase in the density modulation postquench relative to the initial condensate. We find that the relative spectral weight increases to much larger values than those measured in experiment, because we do not account for the finite resolution effects of the imaging system. However, we obtain good quantitative agreement with experiment for the time scales over which the spectral weight grows and subsequently decays [see Fig. 2(b)]. Once fully formed, the droplet crystal is observed to be stable for the lifetime of the system (~300 ms). Droplets gradually evaporate, however, due to three-body loss, and occasionally one is observed to disintegrate once the atom number becomes deficient; such events are typically followed by the recombination of high-density fragments to form a new stable droplet. We also note that a collective breathing mode of the droplet crystal is excited during formation. The rate of atom loss is more rapid (hence shorter lifetime) in the droplet phase than the original condensate because of the significantly higher density.

We have conducted simulations exploring a wide range of parameters, and the values of a_f and κ_3 used above were determined to give a reasonable fit to the experimental results. More information from experiments is necessary to completely determine these parameters. Detailed results for the formation dynamics [see Fig. 2(c)] show that the droplet formation time is sensitive to the value of κ_r. Indeed, the largest value used in Fig. 2(c) leads to a formation time that is at least twice as long as that seen in experiment (as well as leading to too few droplets ~3). We have also explored the effect of changing temperature and find little change in formation time for temperatures up to $T \sim 40$ nK.

We also find that the droplet size and peak density are sensitive to κ_r. This can be simply understood because the droplet forms from the competition between the attractive two-body and the repulsive three-body interactions. The density at which this balance is achieved scales inversely with κ_r. We find that the droplets that form near the center of the trap have very similar properties, including the atom number in each droplet, peak density, transverse ($w_{x,y}$) and axial (w_z) widths, where

$$w_\nu^2 \equiv \gamma N_{\mathrm{D}}^{-1} \int_{\mathrm{D}} d\mathbf{r} \left(r_\nu - r_\nu^{\mathrm{c}}\right)^2 |\psi(\mathbf{r})|^2, \quad \nu = \{x,y,z\}, \qquad (4)$$

with the integration restricted to the region containing the droplet, $\mathbf{r}^{\mathrm{c}}$ the center of the droplet, and N_{D} the number of atoms in the droplet. The factor $\gamma = 8\ln(2)$ is chosen to calibrate this width measure to be the full width at half maximum for Gaussian-shaped droplets. In Table I we show how the properties of the droplets change with the three-body

TABLE I. Droplet properties as κ_r varies for $N_{\mathrm{cond}} = 15 \times 10^3$, $a_f = 82.6 a_0$, with $T = 20$ nK and $\kappa_i = 7.8 \times 10^{-42}\ \hbar\ \mathrm{m}^6/\mathrm{s}$. Evaluated for droplets located within 2.5 μm of the trap center (in the xy plane) using simulation results for $t \geqslant 18$ ms. The error indicates the standard deviation across measured droplets.

κ_r ($10^{-39}\ \hbar\ \mathrm{m}^6/\mathrm{s}$)	N_{D} (10^3)	n_{peak} ($10^{20}\ \mathrm{m}^{-3}$)	$w_{x,y}$ (10^{-6} m)	w_z (10^{-6} m)
3.91	1.2(1)	28(2)	0.26(1)	2.5(2)
5.87	1.5(1)	20(2)	0.33(2)	2.7(1)
7.83	1.8(2)	18(1)	0.36(2)	2.9(2)
9.78	2.0(2)	14(1)	0.42(3)	2.9(2)
11.7	2.4(4)	13(2)	0.46(2)	3.1(2)
19.6	3.4(8)	7(1)	0.60(1)	3.3(2)

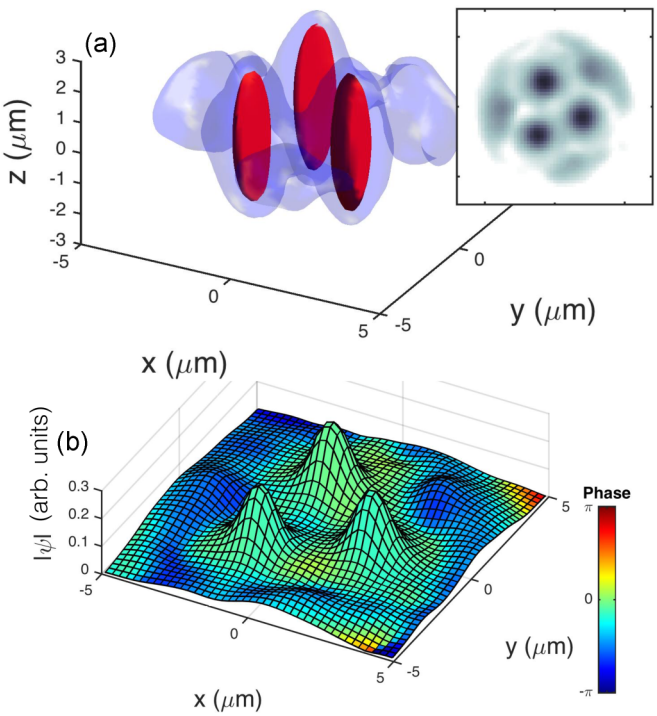

FIG. 3. (Color online) (a) Droplet crystal obtained in our simulations at 15 ms after the quench is started. The red surface indicates a high-density isosurface at $n = 2 \times 10^{20}$ m^{-3} and the blue low-density isosurface is $n = 0.2 \times 10^{20}$ m^{-3}. The inset is a column density made by integrating the density along the z axis. (b) The condensate phase in the $z = 0$ plane. Simulation for 15×10^3 atoms, $\kappa_r = 1.96 \times 10^{-38}\ \hbar$ m^6/s.

interaction. Notably, the droplets get wider and less dense, but hold more atoms, as κ_r increases.

An important area of interest is whether this droplet crystal maintains phase coherence, and hence could be a supersolid [27–29]. This question was not able to be explored in the experiment. We have examined this by analyzing the mean phase of each droplet (the phase varies minimally within each droplet). We find that the first droplets formed have similar phases, which they inherit from the condensate, but in general these quickly become independent. For example, the state shown in Fig. 1 is found to develop independent phases by ∼15 ms after the quench [see Fig. 1(b)]. This occurs due to heating during the droplet formation, e.g., we observe vortex-antivortex pairs created between droplets and the creation of additional phonon excitations. Thus, we predict it is unlikely that the state produced in experiment is a supersolid. However, using a larger value of $\kappa_r = 1.96 \times 10^{-38}\ \hbar$ m^6/s, we have observed the formation of a small droplet crystal in which the phase coherence persists for at least 400 ms [see Fig. 3(b)]. In this case the droplets are approximately twice as wide (see Table I) compared to the case in Fig. 1(b): Only three drops form and the formation time is much slower [∼15 ms—see Figs. 2(c) and 3(a)], and causes less heating. The reduced heating and enhanced tunneling between the larger droplets allows this system to behave as a supersolid.

In conclusion, we have identified the key physical mechanism behind the recent observation of a droplet crystal in a dilute gas of dysprosium. We have investigated properties of the droplets that form and important factors in maintaining phase coherence of the crystal in order to produce a supersolid. Our results show that the crystal produced in experiments was likely not a supersolid because of heating during its rapid formation. In future work we will explore experimentally practical adjustments (changing two-body interactions, trap geometry, etc.) which will enable larger crystals to form in the regime where phase coherence is maintained between the droplets.

Note added. Recently, we became aware of a preprint that also investigates three-body interactions in relation to the formation of a droplet phase in a dipolar condensate [30].

We gratefully acknowledge support from the Marsden Fund of the Royal Society of New Zealand.

[1] H. Kadau, M. Schmitt, M. Wenzel, C. Wink, T. Maier, I. Ferrier-Barbut, and T. Pfau, arXiv:1508.05007.
[2] N. Henkel, R. Nath, and T. Pohl, Phys. Rev. Lett. **104**, 195302 (2010).
[3] F. Cinti, P. Jain, M. Boninsegni, A. Micheli, P. Zoller, and G. Pupillo, Phys. Rev. Lett. **105**, 135301 (2010).
[4] Z.-K. Lu, Y. Li, D. S. Petrov, and G. V. Shlyapnikov, Phys. Rev. Lett. **115**, 075303 (2015).
[5] T. Köhler, Phys. Rev. Lett. **89**, 210404 (2002).
[6] P. J. Everitt, M. A. Sooriyabandara, G. D. McDonald, K. S. Hardman, C. Quinlivan, M. Perumbil, P. Wigley, J. E. Debs, J. D. Close, C. C. N. Kuhn, and N. P. Robins, arXiv:1509.06844.
[7] T. Lahaye, J. Metz, B. Fröhlich, T. Koch, M. Meister, A. Griesmaier, T. Pfau, H. Saito, Y. Kawaguchi, and M. Ueda, Phys. Rev. Lett. **101**, 080401 (2008).
[8] T. Koch, T. Lahaye, J. Metz, B. Froehlich, A. Griesmaier, and T. Pfau, Nat. Phys. **4**, 218 (2008).
[9] R. M. Wilson, S. Ronen, and J. L. Bohn, Phys. Rev. A **80**, 023614 (2009).
[10] S. Müller, J. Billy, E. A. L. Henn, H. Kadau, A. Griesmaier, M. Jona-Lasinio, L. Santos, and T. Pfau, Phys. Rev. A **84**, 053601 (2011).
[11] E. B. Linscott and P. B. Blakie, Phys. Rev. A **90**, 053605 (2014).
[12] C. A. Sackett, H. T. C. Stoof, and R. G. Hulet, Phys. Rev. Lett. **80**, 2031 (1998).
[13] E. A. Donley, N. R. Claussen, S. L. Cornish, J. L. Roberts, E. A. Cornell, and C. E. Wieman, Nature (London) **412**, 295 (2001).
[14] E. A. Burt, R. W. Ghrist, C. J. Myatt, M. J. Holland, E. A. Cornell, and C. E. Wieman, Phys. Rev. Lett. **79**, 337 (1997).
[15] B. Laburthe Tolra, K. M. O'Hara, J. H. Huckans, W. D. Phillips, S. L. Rolston, and J. V. Porto, Phys. Rev. Lett. **92**, 190401 (2004).
[16] T. Maier, H. Kadau, M. Schmitt, M. Wenzel, I. Ferrier-Barbut, T. Pfau, A. Frisch, S. Baier, K. Aikawa, L. Chomaz, M. J. Mark, F. Ferlaino, C. Makrides, E. Tiesinga, A. Petrov, and S. Kotochigova, Phys. Rev. X **5**, 041029 (2015).
[17] E. Braaten, H.-W. Hammer, and T. Mehen, Phys. Rev. Lett. **88**, 040401 (2002).

[18] A. Bulgac, Phys. Rev. Lett. **89**, 050402 (2002).
[19] S. Ronen, D. C. E. Bortolotti, and J. L. Bohn, Phys. Rev. A **74**, 013623 (2006).
[20] A. D. Martin and P. B. Blakie, Phys. Rev. A **86**, 053623 (2012).
[21] P. B. Blakie, A. S. Bradley, M. J. Davis, R. J. Ballagh, and C. W. Gardiner, Adv. Phys. **57**, 363 (2008).
[22] Y. Tang, A. Sykes, N. Q. Burdick, J. L. Bohn, and B. L. Lev, Phys. Rev. A **92**, 022703 (2015).
[23] For $a_f \gtrsim 92a_0$ we do not find any droplets forming within 15 ms, and on longer time scales significantly fewer droplets form than observed in experiment.
[24] L. Santos, G. V. Shlyapnikov, and M. Lewenstein, Phys. Rev. Lett. **90**, 250403 (2003).
[25] S. Ronen, D. C. E. Bortolotti, and J. L. Bohn, Phys. Rev. Lett. **98**, 030406 (2007).
[26] P. B. Blakie, D. Baillie, and R. N. Bisset, Phys. Rev. A **86**, 021604 (2012).
[27] E. Kim and M. H. W. Chan, Nature (London) **427**, 225 (2004).
[28] D. Y. Kim and M. H. W. Chan, Phys. Rev. Lett. **109**, 155301 (2012).
[29] M. Boninsegni and N. V. Prokof'ev, Rev. Mod. Phys. **84**, 759 (2012).
[30] K.-T. Xi and H. Saito, arXiv:1510.07842.